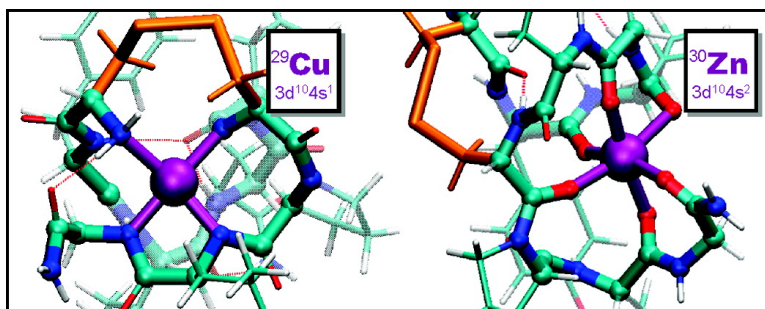Article

Interactions of the Hormone Oxytocin with Divalent Metal Ions

Thomas Wyttenbach, Dengfeng Liu, and Michael T. Bowers

More About This Article

Additional resources and features associated with this article are available within the HTML version:

- Supporting Information
- Access to high resolution figures
- Links to articles and content related to this article
- Copyright permission to reproduce figures and/or text from this article

View the Full Text HTML

Interactions of the Hormone Oxytocin with Divalent Metal Ions

Thomas Wyttenbach, Dengfeng Liu, and Michael T. Bowers*

Department of Chemistry and Biochemistry, University of California, Santa Barbara, Santa Barbara, California 93106

Received January 10, 2008; E-mail: bowers@chem.ucsb.edu

Abstract: The interaction of the cyclic nonapeptide oxytocin (OT) with a number of alkaline earth and divalent transition metal ions (X^{2+}) was examined employing mass spectrometry (MS) and ion mobility spectrometry (IMS) techniques in combination with molecular dynamics (MD) and density functional theory (DFT) calculations. Under acidic conditions it was found that OT exhibits an exceptionally strong affinity for all divalent metal ions resulting in strong $[OT + X]^{2+}$ peaks in the mass spectrum. Under basic conditions only Cu^{2+} and Ni^{2+}−OT complexes were detected and these were singly, doubly, triply, or quadruply deprotonated. Collision-induced dissociation of the $[OT - 3H + Cu]^-$ complex yielded exclusively C-terminal Cu^{2+}-containing fragments ($Cu^{2+}fragment^{3-}$), suggesting that the Cu^{2+} ligation site includes deprotonated C-terminal backbone amide nitrogen atoms and the N-terminal amino nitrogen atom in $[OT - 3H + Cu]^-$. MD and DFT calculations indicate a square-planar complex is consistent with these observations and with experimental collision cross sections. MD and DFT calculations also indicate either an octahedral or trigonal-bipyramidal complex between Zn^{2+} and OT is lowest in energy with carbonyl oxygens being the primary ligation sites. Both complexes yield cross sections in agreement with experiment. The biological impact of the structural changes induced in OT by divalent metal ion coodination is discussed.

Introduction

Metal ion–peptide systems have attracted researchers with an interest at the interface between inorganic chemistry and biochemistry for more than half a century. The comprehensive review by Sigel and Martin gives an excellent overview of the earlier work in the field.[1] Metal ions are essential components in biochemical systems carrying out a range of functions as important as catalyzing biochemical reactions in enzymes and assisting in the oxygen transport in hemoglobin. Research on simple metal−peptide systems provides a basis for understanding metal interactions occurring in biochemically relevant systems. In addition, the chemistry of transition metal−peptide interactions is an interesting field of research in its own right, independent of the biological relevance of simple metal−peptide complexes.[1]

With the development of ionization techniques suitable for interrogation of biomolecules by mass spectrometry (MS)[2–5] research of metal−peptide systems began to expand into the field of solvent-free chemistry[6–16] including studies on metal−oxytocin complexes.[10,15,16] The peptide oxytocin (OT) belongs to a group of neurohypophysial hormones present in virtually all vertebrates and many other species as primitive as the earthworm *Eisenia fetida*.[17] The neurohypophysial hormones,

all of them nonapeptides with a disulfide bridge between Cys residues 1 and 6 (Scheme 1), can be classified into the OT and vasopressin (VP) families based on the nature of residue 8. The OT family contains a neutral amino acid in position 8, vasopressins a basic amino acid (Arg or Lys). Virtually all vertebrate species possess an OT-like and a VP-like peptide each with a different receptor and a different function. The two neurohypophysial hormones of bony fishes, believed to be predecessors of the land vertebrates, are isotocin (IT) and vasotocin (VT) with the sequences shown in Table 1 along with the sequences of OT and VP found in humans and many other mammals. OT is associated with reproductive functions, the stimulation of uterine contractions during labor and milk ejection during lactation, whereas VP facilitates water reabsorption by the kidney and the contraction of smooth muscle cells in arteries.

(1) Sigel, H.; Martin, R. B *Chem. Rev.* **1982**, *82*, 385–426.
(2) Barber, M.; Bordoli, R. S.; Sedgwick, R. D.; Tyler, A. N. *J. Chem. Soc., Chem. Commun.* **1981**, 325–327.
(3) Bahr, U.; Karas, M.; Hillenkamp, F. *Fresenius' J. Anal. Chem.* **1994**, *348*, 783–791.
(4) Tanaka, K. *Angew. Chem., Int. Ed.* **2003**, *42*, 3860–3870.
(5) Fenn, J. B. *Angew. Chem., Int. Ed.* **2003**, *42*, 3871–3894.
(6) Hu, P. F.; Gross, M. L. *J. Am. Chem. Soc.* **1993**, *115*, 8821–8828.
(7) Reiter, A.; Adams, J.; Zhao, H. *J. Am. Chem. Soc.* **1994**, *116*, 7827–7838.
(8) Loo, J. A.; Hu, P. F.; Smith, R. D. *J. Am. Soc. Mass Spectrom.* **1994**, *5*, 959–965.
(9) Masselon, C.; Salih, B.; Zenobi, R. *J. Am. Soc. Mass Spectrom.* **1999**, *10*, 19–26.
(10) Wei, H.; Luo, X. M.; Wu, Y. B.; Yao, Y.; Guo, Z. J.; Zhu, L. G. *J. Chem. Soc., Dalton Trans.* **2000**, 4196–4200.
(11) Vaisar, T.; Gatlin, C. L.; Rao, R. D.; Seymour, J. L.; Turecek, F. *J. Mass Spectrom.* **2001**, *36*, 306–316.
(12) Williams, S. M.; Brodbelt, J. S. *J. Am. Soc. Mass Spectrom.* **2004**, *15*, 1039–1054.
(13) Chitta, R. K.; Gross, M. L. *Biophys. J.* **2004**, *86*, 473–479.
(14) Ross, A. R. S.; Luettgen, S. L. *J. Am. Soc. Mass Spectrom.* **2005**, *16*, 1536–1544.
(15) Liu, D. F.; Seuthe, A. B.; Ehrler, O. T.; Zhang, X. H.; Wyttenbach, T.; Hsu, J. F.; Bowers, M. T. *J. Am. Chem. Soc.* **2005**, *127*, 2024–2025.
(16) Kleinnijenhuis, A. J.; Mihalca, R.; Heeren, R. M. A.; Heck, A. J. R. *Int. J. Mass Spectrom.* **2006**, *253*, 217–224.
(17) Oumi, T.; Ukena, K.; Matsushima, O.; Ikeda, T.; Fujita, T.; Minakata, H.; Nomoto, K. *Biochem. Biophys. Res. Commun.* **1994**, *198*, 393–399.

Scheme 1. Chemical Structure and CID Fragments x_n and z_4 of Oxytocin
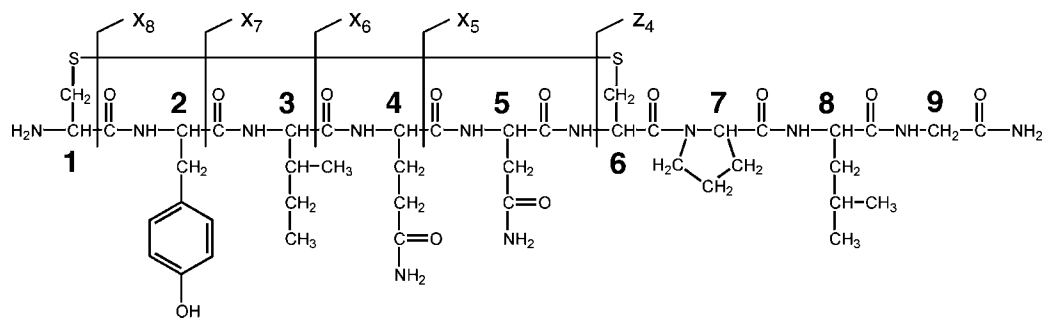
Table 1. Amino Acid Sequence of Some Oxytocin and Vasopressin Peptides

	1	2	3	4	5	6	7	8	9
oxytocin(OT)	Cys	Tyr	Ile	Gln	Asn	Cys	Pro	Leu	Gly(NH₂)
isotocin(IT)	Cys	Tyr	Ile	Ser	Asn	Cys	Pro	Ile	Gly(NH₂)
vasopressin(VP)	Cys	Tyr	Phe	Gln	Asn	Cys	Pro	Arg	Gly(NH₂)
vasotocin(VT)	Cys	Tyr	Ile	Gln	Asn	Cys	Pro	Arg	Gly(NH₂)

Many aspects of the OT system including behavioral effects mediated or modulated by OT, physiological regulation by steroids, and the functions of OT-like hormones in nonmammalians are poorly understood.[18] Information about the three-dimensional shape of the receptors, members of the family of G protein-coupled receptors, is sketchy since membrane proteins are inherently difficult to study in atomic detail in their native environment.[18,19]

Divalent metal ions appear to be another important element of the OT system. It was reported that the hormone−receptor binding was potentiated in the presence of certain divalent metal ions such as Mg^{2+}, Mn^{2+}, Co^{2+}, Ni^{2+}, and Zn^{2+}, whereas other metal ions such as Ca^{2+}, Fe^{2+}, and Cu^{2+} had no effect.[20] While research on the structure of the OT receptor (OTR), including studies involving the interaction with metal ions, is extremely difficult, a number of researchers have focused on investigating the interaction of metal ions with OT itself. Photospectrometric and potentiometric studies on metal−OT complexes[21-26] were pioneered by Breslow nearly 50 years ago.[21]

Here we report results of experiments employing MS and ion mobility techniques in combination with theoretical molecular dynamics (MD) and density functional theory (DFT) calculations. This study follows our previous communication[15] of first results on Zn^{2+}−OT[15] and is a full account including the peptides OT, IT, VP, and VT (Table 1) and the biologically relevant and chemically interesting divalent metal ions Mg^{2+}, Ca^{2+}, Mn^{2+}, Co^{2+}, Ni^{2+}, Cu^{2+}, and Zn^{2+}.

Methods

The experimental work presented here comprises collision cross section and collision-induced dissociation (CID) studies. The two types of experiments were carried out on two different instruments briefly described below along with sample preparation techniques. These descriptions are followed by an outline of the theoretical methods employed here to calculate model structures.

Collision Cross Sections. The custom-built ion mobility mass spectrometer employed to measure collision cross sections has previously been described in detail.[27] Briefly, ions are formed by electrospray ionization (ESI) and transferred into a high-vacuum chamber by an ion funnel, which is also used to convert the continuous beam of ions from the source into short pulses of ions. The ion pulses are injected into a drift cell filled with 5 Torr of helium. Ions are pulled through the cell under the influence of a weak electric field. Ions exiting the cell are mass selected in a quadrupole mass filter and detected as a function of their arrival time. To ensure optimum signal intensity in these experiments the mass resolution is kept relatively low ($m/\Delta m = 100$–200), not sufficient to resolve individual isotope peaks, but high enough to separate bare OT from the metal−OT complex. From the ion arrival time distribution (ATD) and from the known drift length, drift field, and helium pressure the ion−helium collision cross section can be calculated providing information about the shape of the polyatomic ion.[28,29] Cross section measurements are reproducible within 1%. An ATD width given by the instrument resolution was observed in all experiments, indicating that only one type of ion structure is present or that interconversion between different types of structures is rapid on the experimental time scale of 1 ms.

Collision-Induced Dissociation. Collision-induced dissociation experiments were carried out on a commercial quadrupole-time-of-flight (Q-TOF) mass spectrometer (Waters Micromass Q-TOF-2, Manchester, U.K.). Sample introduction to the Z-spray at +3.5 kV and −3.0 kV spray voltage for positive and negative ions, respectively, occurs through an infusion pump at a flow rate of 5 μL min^{-1}. Ions are mass selected in a quadrupole mass filter (with a resolution similar to the cross section experiments, see above) and subsequently subjected to 25–40 V collisions with argon in the collision cell. The resulting fragment ions are then analyzed in the orthogonal reflectron TOF mass spectrometer. All mass spectra shown here were recorded on the Q-TOF spectrometer.

Sample Preparation. OT was purchased from SynPep (Dublin, California), IT, VT, and VP from Sigma-Aldrich (St. Louis, Missouri). All metal salts are high-purity crystal grade, solvents are HPLC grade. Electrospray solutions prepared by dissolving the peptides (50 μM) and metal salts (50 μM) in a 1:1 mixture of water and acetonitrile produced a more stable spray and better signal than pure water solutions and yielded qualitatively the same results as

(18) Gimpl, G.; Fahrenholz, F. *Physiol. Rev.* **2001**, *81*, 629–683.
(19) Fanelli, F.; Barbier, P.; Zanchetta, D.; De Benedetti, P. G.; Chini, B. *Mol. Pharmacol.* **1999**, *56*, 214–225.
(20) Pearlmutter, A. F.; Soloff, M. S. *J. Biol. Chem.* **1979**, *254*, 3899–3906.
(21) Breslow, E. *Biochim. Biophys. Acta* **1961**, *53*, 606–609.
(22) Campbell, B. J.; Chu, F. S.; Hubbard, S. *Biochemistry* **1963**, *2*, 764–&.
(23) Kozlowski, H.; Radomska, B.; Kupryszewski, G.; Lammek, B.; Livera, C.; Pettit, L. D.; Pyburn, S. *J. Chem. Soc., Dalton Trans.* **1989**, 173–177.
(24) Bal, W.; Kozlowski, H.; Lammek, B.; Pettit, L. D.; Rolka, K. *J. Inorg. Biochem.* **1992**, *45*, 193–202.

(25) Danyi, P.; Varnagy, K.; Sovago, I.; Schon, I.; Sanna, D.; Micera, G. *J. Inorg. Biochem.* **1995**, *60*, 69–78.
(26) Chruscinska, E.; Derdowska, I.; Kozlowski, H.; Lammek, B.; Luczkowski, M.; Oldziej, S.; Swiatek-Kozlowska, J. *New J. Chem.* **2003**, *27*, 251–256.
(27) Wyttenbach, T.; Kemper, P. R.; Bowers, M. T. *Int. J. Mass Spectrom.* **2001**, *212*, 13–23.
(28) Wyttenbach, T.; Bowers, M. T. *Top. Curr. Chem.* **2003**, *225*, 207–232.
(29) Mason, E. A.; McDaniel, E. W. *Transport Properties of Ions in Gases*; Wiley: New York, 1988.

pure aqueous solutions (see Supporting Information). Water−acetonitrile solutions were used for spectra shown in all figures unless otherwise noted. Solvents including 1% acetic acid yielded a pH of 3.0, solvents with 1% NH₄OH, a pH of 10.3. Neutral solutions (pH 7.0) were buffered by 1 mM ammonium acetate.

Theoretical Model Structures. Model structures of complexes were obtained by a procedure including molecular modeling to search conformational space and electronic structure calculations for geometry refinement and more accurate energetics. The conformational search was based on a simulated annealing protocol similar to that previously applied to peptides[30] including OT (see Supporting Information of ref 15). The AMBER 7 suite of programs was used for the MD calculations including the AMBER force field ff99.[31] X^{2+} ions chelated by neutral peptides were modeled as simple charge centers that were free to move to any ligating group present on the peptide. For the Cu^{2+} ion chelated by an anionic peptide a special force field was developed including co-valent $Cu^{2+}-NH_2$ and $Cu^{2+}-N^-$ bonds, $NH_2-Cu^{2+}-N^-$ and $N^--Cu^{2+}-N^-$ angles with potential minima at 90° and 180°, and $C_\alpha-NH_2-Cu^{2+}-N^-$ and $C_\alpha-N^--Cu^{2+}-N^-$ dihedral angles with potential minima at multiples of 180°. The force constants for bonds and angles and the barrier heights for dihedrals involving Cu^{2+} were set to arbitrary high values resulting in a rigid copper-chelate moiety. Employing this force field was the only approach yielding metal−peptide complexes with a square-planar metal coordination geometry which could be used as reasonable starting structures for electronic structure calculations.

Electronic structure calculations on selected low-energy AMBER structures were performed using the JAGUAR 5.0 software package.[32] The calculations are based on DFT and employ the B3LYP hybrid functional[33,34] with the LACVP and LACV3P basis sets[32] which include effective core potentials for the heavy atoms (Cu, Zn)[35] and the 6-31G and 6-311G basis sets, respectively, for the lighter atoms (H, C, N, O, S).[36,37] The effect of added polarization functions on all atoms (LACVP**) was studied on selected examples, as was the effect of diffuse functions on all atoms except hydrogen in anionic systems (LACVP+**). All structures were fully geometry optimized at the B3LYP/LACVP level of theory until converged to a root-mean-square value of energy gradient and nuclear displacement of 9.0×10^{-4} hartree $bohr^{-1}$ and 1.2×10^{-3} bohr, respectively. The more expensive LACV3P and LACVP**, calculations (with 1100 and 1300 basis functions, respectively) were converged to 1.5×10^{-3} hartree $bohr^{-1}$ and 6.0×10^{-3} bohr, LACVP+** calculations (1600 basis functions) to 6×10^{-3} hartree $bohr^{-1}$ and 1.4×10^{-2} bohr. Structures presented in figures were prepared using the VMD graphics software, version 1.8.1.[38]

For the doublet states of Cu^{2+}-containing open-shell systems unrestricted DFT (UDFT) calculations were carried out. A comparison with a restricted open-shell B3LYP/LACVP calculation (RODFT) for the square-planar $[Gly_3-NH-CH_3 - 3H + Cu]^-$ model system yields slightly higher energies (by 0.6 kcal mol) for RODFT compared to UDFT. A natural bond orbital (NBO) analysis of the same model system yields a natural charge of +1.14 on the copper atom. This charge of >1 agrees with a formal Cu^{II} oxidation state, indicating the geometry optimization occurred on the surface
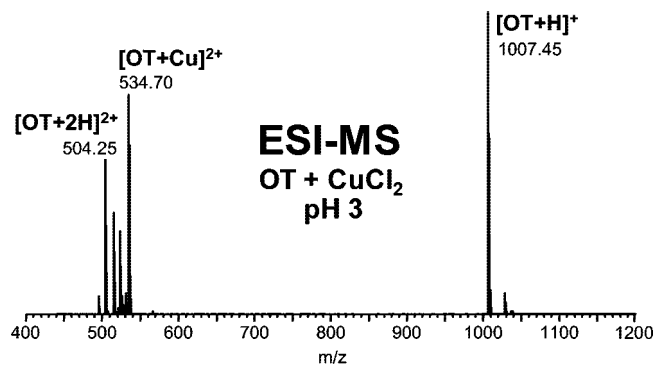
(30) Wyttenbach, T.; von Helden, G.; Bowers, M. T. *J. Am. Chem. Soc.* **1996**, *118*, 8355−8364.

(31) Case, D. A.; et al. *Amber 7*, University of California: San Francisco, 2002.

(32) *Jaguar*, 5.0; Schrodinger, L.L.C.: Portland, 1991−2003.

(33) Becke, A. D. *J. Chem. Phys.* **1993**, *98*, 5648−5652.

(34) Lee, C. T.; Yang, W. T.; Parr, R. G. *Phys. Rev. B* **1988**, *37*, 785−789.

(35) Hay, P. J.; Wadt, W. R. *J. Chem. Phys.* **1985**, *82*, 299−310.

(36) Hehre, W. J.; Ditchfield, R.; Pople, J. A. *J. Chem. Phys.* **1972**, *56*, 2257−2261.

(37) Krishnan, R.; Binkley, J. S.; Seeger, R.; Pople, J. A. *J. Chem. Phys.* **1980**, *72*, 650−654.

(38) Humphrey, W.; Dalke, A.; Schulten, K. *J. Mol. Graphics* **1996**, *14*, 33−&.

Figure 1. Electrospray mass spectrum of an aqueous solution of 50 μM oxytocin, 50 μM $CuCl_2$, and 200 mM acetic acid (pH 3).

of the correct electronic state. The three deprotonated amide groups carry a natural charge of −0.86, −0.81, −0.88, respectively.

The cross sections of the theoretical structures were obtained using a projection model approximation.[39] For systems with known structures this type of calculation yields cross sections that deviate from experiment generally by <2%.[39] For complex systems such as peptides where numerous rapidly interconverting structures may be populated under thermal conditions the *average* cross section is expected to agree with experiment within <2%. Previous calculations on $[OT + H]^+$ and $[OT + Zn]^{2+}$ indicate that agreement between experiment and *one* selected representative structure is expected within 3% (see Supporting Information of ref 15).

Results and Discussion

Strong $[OT + X]^{2+}$ signals were obtained for all divalent metal ions X^{2+}. An example is given in Figure 1 showing a mass spectrum of a 50 μM acidic (pH 3) aqueous solution of OT and $CuCl_2$ with the main features corresponding to singly and doubly protonated OT and to the copper−OT complex. Similar spectra are obtained for the peptides IT, VP, VT and for other divalent metal ions $(Mg^{2+}, Ca^{2+}, Mn^{2+}, Ni^{2+}, Co^{2+}, Zn^{2+})$. (See Supporting Information.)

Figure 2 shows a mass spectrum of a mixture of several divalent metal ions (each at 50 μM) competing for the OT ligand under acidic conditions. Whereas the spectrum indicates a slightly increased affinity of OT for Mg^{2+} and Ca^{2+}, the hormone binds to every type of metal ion present. If the same solution of OT and metal salts is buffered at pH 10, the only divalent metal ion observed in the mass spectrum to form complexes with OT is copper (Figure 3). The general absence of metal−OT complexes is not unexpected because in the pH 10 region competition from hydroxo complex formation is severe, and the question is how the $Cu^{2+}-$OT complex is able to win over $Cu^{2+}(OH^-)_n$. Close examination of the mass spectrum of Figure 3 indicates that OT is deprotonated in all of the copper-containing species with loss of up to three protons $([OT - 3H + Cu + 3 Na]^{2+})$.

The corresponding negative ion spectrum is shown in Figure 4. Again, none of the divalent metal ions are observed to form complexes with OT except Cu^{2+}. The most intense peak corresponds to the triply deprotonated OT ligand bound to Cu^{2+} $([OT - 3H + Cu]^-)$. A small amount of $[OT - 4H + Cu]^{2-}$ is also evident. The ATD shown in the inset is typical of all ATDs observed in this work: a single narrow peak (see Supporting Information). Figure 5 shows mass spectra obtained for mixtures of OT with $CoCl_2$ (Figure 5a), $NiCl_2$ (Figure 5b), and $ZnCl_2$

(39) Wyttenbach, T.; von Helden, G.; Batka, J. J.; Carlat, D.; Bowers, M. T. *J. Am. Soc. Mass Spectrom.* **1997**, *8*, 275−282.
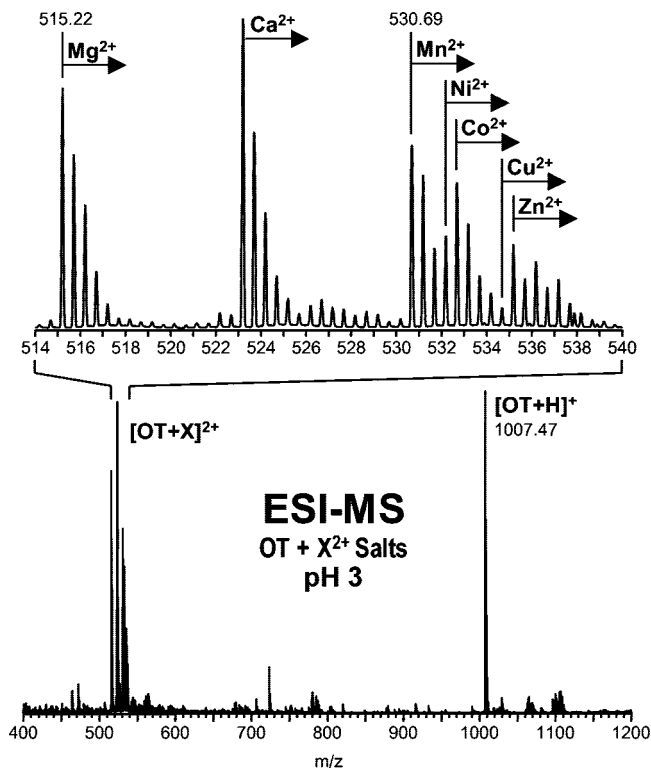
Figure 2. Electrospray mass spectrum of an acidic (pH 3) solution of oxytocin, MgSO$_4$, CaCl$_2$, MnCl$_2$, CoCl$_2$, NiCl$_2$, CuCl$_2$, and ZnCl$_2$ (each at 50 μM). The blow up of m/z 514–540 shows groups of peaks corresponding to the metal and carbon isotopic distributions of the various [OT + X]$^{2+}$ complexes.
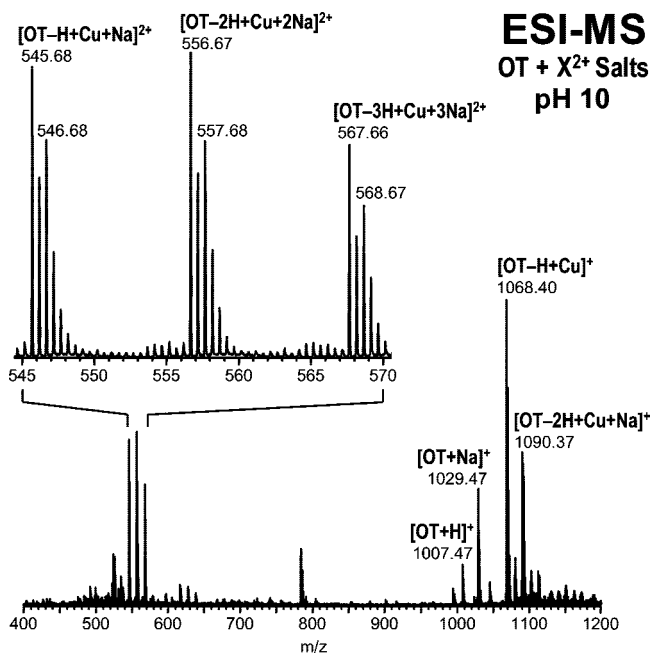

Figure 3. Electrospray mass spectrum of a basic (pH 10) solution of oxytocin, MgSO$_4$, CaCl$_2$, MnCl$_2$, CoCl$_2$, NiCl$_2$, CuCl$_2$, and ZnCl$_2$ (each at 50 μM).

(Figure 5c), the neighbors of copper in the periodic table ($_{27}$Co, $_{28}$Ni, $_{29}$Cu, $_{30}$Zn). Whereas complexes are completely absent in the Co^{2+} and Zn^{2+} spectra, for Ni^{2+} there is a small amount of [OT $-$ 3H + Ni]$^-$ and [OT $-$ 4H + Ni]$^{2-}$ observed. However, the spectrum of competing metal ions in Figure 4 indicates that Cu^{2+} ions bind much more strongly to OT than Ni^{2+}.
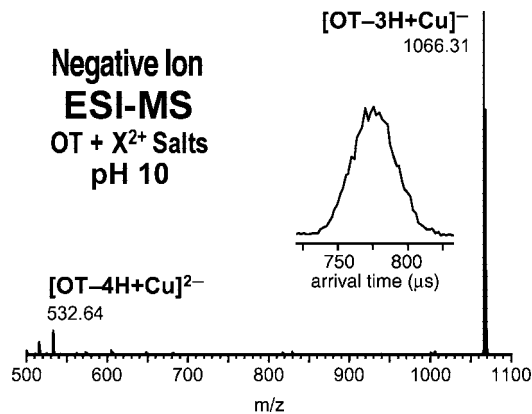
Figure 4. Negative ion electrospray mass spectrum of a basic (pH 10) solution of oxytocin, MgSO$_4$, CaCl$_2$, MnCl$_2$, CoCl$_2$, NiCl$_2$, CuCl$_2$, and ZnCl$_2$ (each at 50 μM). The inset shows the ATD of the mass-selected [OT $-$ 3H + Cu]$^-$ ion.

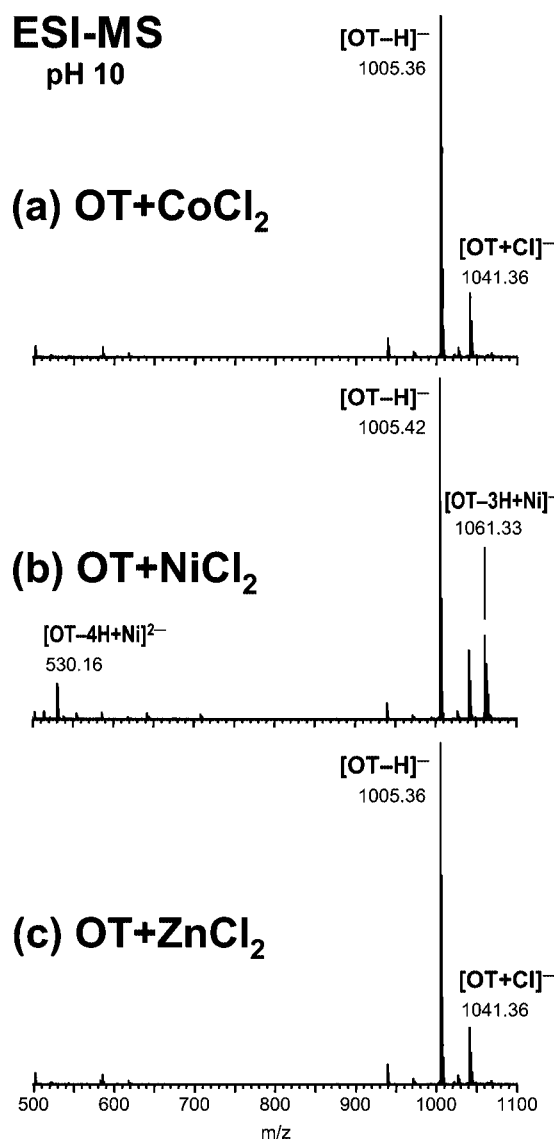**Figure 5.** Negative ion electrospray mass spectrum of a basic (pH 10) solution of 50 μM oxytocin and 50 μM (a) CoCl$_2$, (b) NiCl$_2$, and (c) ZnCl$_2$.

The increasing propensity $_{27}$Co, $_{30}$Zn $<$ $_{28}$Ni $<<$ $_{29}$Cu for forming metal$-$OT complexes with loss of up to four protons at pH 10 raises questions such as which OT sites are deproto-

nated and how OT interacts with metal ions. OT is a peptide without carboxyl groups. The most acidic group in OT, the Tyr[2] side chain, has a pK_a of 10.1 with the other proton-containing groups, the $-CONH-$ backbone amides, the $-CONH_2$ amides of Gln[4], Asp[5], and Gly[9], and the N-terminal $-NH_2$ amino group, having significantly higher pK_a values.[40,41]

The review by Sigel and Martin[1] addresses the question of the metal$-$amide interaction and indicates that divalent metal ions bind to the amide oxygen atom (**1**). However, if the amide group is anionic due to deprotonation, metal interaction occurs at the nitrogen atom (**2**). Since the $-NH-$ group of amides is only weakly acidic (pK_a 15), metal ions are expected to bind to the amide oxygen atom near pH 7. However, it has been observed that certain metal ions such as Ni^{2+} and especially Cu^{2+} are able to promote amide deprotonation even at pH < 7.[1,21,42–50] For instance, for the copper(II)$-$diglycine complex a pK_a value of 4 is observed for amide deprotonation.[44] The pK_a values for the corresponding Ni^{2+}, Co^{2+}, and Zn^{2+} oligoglycine complexes are 8, 10, and >10, respectively.[1,45–47] Whereas amide proton displacement is observed for Cu^{2+} and Ni^{2+} and in selected cases for Co^{2+} at pH $\geq$ 10, amide deprotonation generally does not occur in zinc(II)$-$peptide complexes.[1]


1   **2**
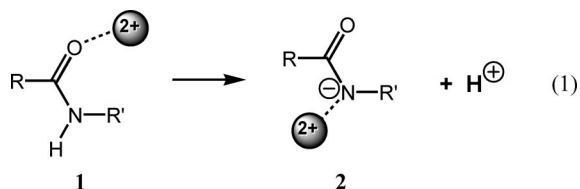
The abundance of X^{2+} metal ions ligated by deprotonated OT observed in our mass spectra (Figures 3$-$5) follows qualitatively the same trend established for oligoglycines. For Cu^{2+} we observe strong peaks corresponding to complexes of deprotonated OT (Figures 3 and 4), Ni^{2+} is able to deprotonate OT (Figure 5b) but loses the competition for the ligand in the presence of copper (Figure 4), and Co^{2+} and Zn^{2+} do not deprotonate OT at all at pH 10 (a and c of Figure 5). These results indicate that the transition metal$-$OT complexes detected in the mass spectrometer are formed in solution and that the state of OT protonation in these complexes does not change during the electrospray process. Whether mass spectrometry can be applied to obtain solution-phase information of metal–ligand systems appears to be system dependent as concluded in a recent review.[51]

3
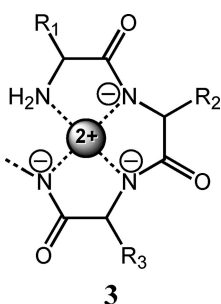
For small oligoglycine systems nickel and copper are able to displace up to three protons by forming quasi-planar metal$-$peptide

complexes (**3**).[1,48,49] In these complexes the metal ion is bound to the neutral N-terminal amino group which is considered the anchor initiating chelation to the nitrogen atoms of three deprotonated amide groups (4N chelation). A comparison of chelation properties of α-amino acids with those of β-amino acids indicates that five-membered chelate rings (such as those of **3**) are particularly favorable. The titration curves of the copper(II)$-$OT system follow closely those of oligoglycines and indicate loss of four protons in the pH range 5–8, corresponding to neutralization of the N-terminal amino group (eq 2) and three-fold amide deprotonation (eq 1).[21] Absorption spectra of basic copper$-$OT solutions[21] show an absorption maximum and extinction coefficient nearly identical to that of the corresponding copper$-$tetraglycine system[50] suggesting similar structures for $Cu^{2+}-Gly_4$ and $Cu^{2+}-OT$. A fifth proton stemming from the tyrosine hydroxyl group is lost at pH 10 (eq 3).[21]

$$ \qquad (2) $$

$$ \qquad (3) $$
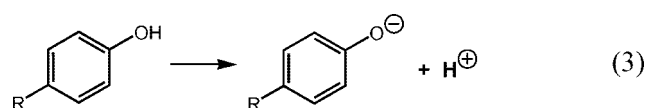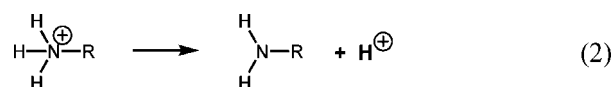
Metal complexes of triply deprotonated OT are apparent in our pH 10 mass spectra of OT in the presence of Ni(II) and Cu(II) salts (Figures 3–5) suggesting structures analogous to **3**. Even 4-fold OT deprotonation is observed in nickel and copper complexes (Figures 4 and 5b) indicating additional loss of the tyrosine proton in these cases.

If we mass-select the triply deprotonated species $[OT - 3H + Cu]^-$ seen in Figure 4 and subsequently perform a collision-induced dissociation (CID) experiment we obtain the fragmentation spectrum displayed in Figure 6. The blow-up of a fragment peak shown in the inset of Figure 6 is representative for all fragments labeled in the spectrum and shows the characteristic pattern expected for compounds containing a copper atom in the natural $^{63}Cu/^{65}Cu$ isotope ratio of 2:1 (overlapping with the $^{12}C-^{13}C$ distribution). No fragments are observed in the 100–400 mass range. The result that CID leads exclusively to copper-containing ionic fragments indicates that the three anionic amide groups stay with the fragment ligating the copper ion (Scheme 2).

Two of the most intense peaks in the CID spectrum observed for all of the OT, IT, VP, and VT peptides (all with sequence Cys-Tyr-x-x-Asn-Cys-Pro-x-Gly) correspond to loss of 74 and 237 amu from the parent ion (see Supporting Information for all CID MS data). These two features, for OT at $m/z = 992$ and 829, respectively (Figure 6), can be assigned to $x_8 + H$

(40) Lide, D. R., *CRC Handbook of Chemistry and Physics*, 87th ed.; CRC: Boca Raton, FL, 2006.

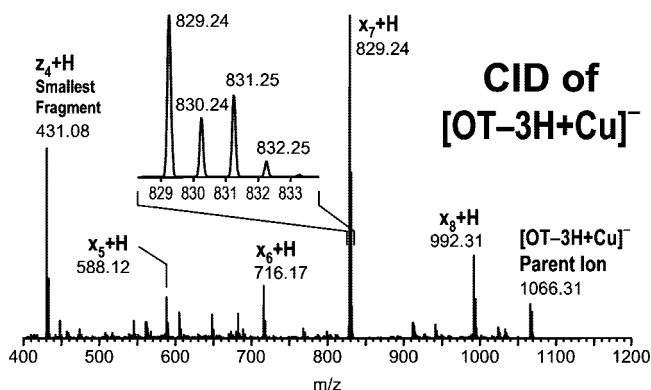(41) Branch, G. E. K.; Clayton, J. O. *J. Am. Chem. Soc.* **1928**, *50*, 1680–1686.

(42) Dobbie, H.; Kermack, W. O. *Biochem. J.* **1955**, *59*, 257–264.

(43) Datta, S. P.; Rabin, B. R. *T. Faraday Soc.* **1956**, *52*, 1123–1130.

(44) Sigel, H. *Inorg. Chem.* **1975**, *14*, 1535–1540.

(45) Martin, R. B.; Chamberlin, M.; Edsall, J. T. *J. Am. Chem. Soc.* **1960**, *82*, 495–498.

(46) Michailidis, M. S.; Martin, R. B. *J. Am. Chem. Soc.* **1969**, *91*, 4683–4689.

(47) Dorigatti, T. F.; Billo, E. J. *J. Inorg. Nucl. Chem.* **1975**, *37*, 1515–1520.

(48) Freeman, H. C.; Taylor, M. R. *Acta Crystallogr.* **1965**, *18*, 939–952.

(49) Blount, J. F.; Freeman, H. C.; Holland, R. V.; Milburm, G. H. *J. Biol. Chem.* **1970**, *245*, 5177–5185.

(50) Koltun, W. L.; Roth, R. H.; Gurd, F. R. N. *J. Biol. Chem.* **1963**, *238*, 124–131.

(51) Di Marco, V. B.; Bombi, G. G. *Mass Spectrom. Rev.* **2006**, *25*, 347–379.

Figure 6. Negative ion CID mass spectrum of the mass-selected [OT − 3H + Cu]⁻ species (50 μM oxytocin, 50 μM CuCl₂, pH 10). The inset shows the isotope distribution of the $x_7 + H$ fragment primarily due to the presence of the ¹²C, ¹³C, ⁶³Cu, and ⁶⁵Cu isotopes. Similar distributions are found for all $x_n + H$ and $z_4 + H$ fragments (and the parent ion).

Scheme 2. CID reaction channels of [OT − 3H + Cu]⁻.
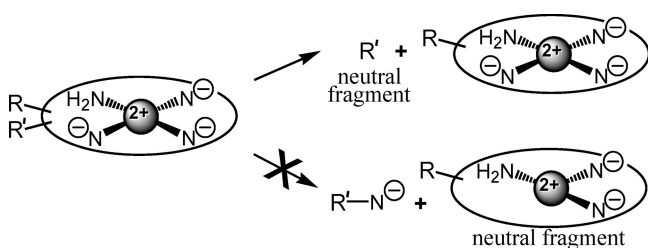
and $x_7 + H$ ions corresponding to loss of Cys¹ and Tyr² (Scheme 1). The $x_n + H$ notation indicates the x_n fragment carrying a charge of −1 (Cu²⁺ − 3H⁺) is hosting an additional H• atom. Observation of intense x fragment peaks is rather unusual in peptide CID experiments. Usually fragmentation occurs at the CO−NH peptide bond yielding y fragments. However, x-type fragmentation has previously been observed for di and tripeptides chelating divalent transition metal ions[6,52] suggesting that cleavage of the Cα−CO bond is promoted by the transition metal ion. The previous work including isotopically labeled peptides[6,52] leads to the mechanism proposed in scheme 3 for loss of the N-terminal residue. Similar mechanisms are presumably responsible for sequential loss of N-terminal amino acids leading to the observed $x_n + H$ fragments in Figure 6. Plausible mechanisms are given in Supporting Information along with a brief introduction to relevant studies available in the literature.[6,52–57]

The smallest fragment with high abundance, at $m/z = 431$ for the OT family of peptides (OT and IT) and $m/z = 474$ for the VP family (VP and VT), respectively, can be assigned to a $z_4 + H$ ion (scheme 1), containing residues 6–9. For the two families of peptides residues 6–9 differ only in residue 8 with the oxytocins possessing Leu⁸/Ile⁸ and the vasopressins Arg⁸. Leu and Arg differ in mass by 43 amu, thus explaining the mass difference in the $z_4 + H$ fragments of the two families. A

plausible mechanism for formation of the $z_4 + H$ fragment is also given in Supporting Information.[6,52–57]

The CID data are unambiguous on several points. First, the Cu²⁺ ion remains with each fragment ion observed indicating that each fragment is triply deprotonated. Second, sequential loss of "N-terminal" residues occurs. Third, the smallest fragment is the $z_4 + H$ ion, a triply deprotonated fragment containing residues 6–9 (Cys-Pro-Leu-Gly–NH₂) ligating Cu²⁺. The most straightforward interpretation of these data is that the original ligation of Cu²⁺ by the intact OT peptide in solution occurs with deprotonated amide moieties associated with Leu⁸ and Gly⁹ and one additional anionic site. There are two sites most strongly suggested by the data: the amide associated with Cys⁶ and the "second" amide associated with Gly⁹−NH₂. This possible set of amide nitrogen deprotonation sites, labeled 3N₆₈₉ and 3N₈₉₉, provide a starting point for performing calculations.

A further piece of information is also useful. Since small oligoglycines form triply deprotonated complexes with Cu²⁺ that are tetracoordinate and quasi-planar and since copper(II)−OT closely follows titration curves of the copper(II)−oligoglycine systems, then it is reasonable that copper(II)−OT is tetracoordinate in solution.[1,21,48–50] In the oligoglycines the N-terminal amino group is the fourth nitrogen coordinated. Hence, we expand the copper(II)−OT coordination to include this nitrogen center, and our starting structures are now 4N₁₆₈₉ and 4N₁₈₉₉. Using procedures described in detail in the section Theoretical Model Structures, MD was employed to generate candidate structures, and then DFT was used to refine these structures and obtain relative energies. From the final structures, cross sections could be calculated to compare with experiment. These structures are given in panels (a) and (b) in Figure 7 and energies and cross sections collected in Table 2. The bottom line is that 4N₁₆₈₉ is at significantly lower energy than 4N₁₈₉₉ and its more compact shape agrees much better with experiment than the more elongated structure of 4N₁₈₉₉. The <3% difference between cross sections of experiment and theory for 4N₁₆₈₉ is acceptable, given the difficulty of accurately calculating structures of transition metal ions bound to a peptide of this size.

The arguments made here for the structure of the very stable [OT − 3H + Cu]⁻ system in basic solution are meant to provide options consistent with all of the observed data. The 4N₁₆₈₉ structure in Figure 7a meets these consistency criteria. The arguments are not meant to provide definitive proof. In Supporting Information theoretical data is given on other systems as we carefully searched all reasonable options. One of these species, 4N₁₂₃₄, is predicted to be at lower energy than the favored 4N₁₆₈₉ coordination, but its cross section is unacceptably too large, and deprotonatin of N-terminal residues in the intact Cu²⁺−OT peptide would require significant charge rearrangement for each residue lost in the CID experiment, a very unlikely scenario. A more thorough examination of the entire [OT − 3H + Cu]⁻ potential surface is well beyond the scope of this work.

At pH < 4 the copper ion is not able to deprotonate amide groups. Hence, at acidic pH copper is ligated by the amide oxygen atom (**1**) similar to all other divalent metal ions. Our previous molecular modeling work on [OT + Zn]²⁺ indicated that the Zn²⁺ ion coordinates six backbone C=O groups (Figure 8a) in a near-octahedral coordination sphere (6O chelation) with C=O···Zn²⁺ distances of ~2.1 Å.[15] Additional modeling work in this study supports the octahedral coordination geometry, but indicates that the N-terminal amino group is also a competitive ligand. A slightly lower-energy [OT + Zn]²⁺ structure is found

(52) Hu, P. F.; Gross, M. L. *J. Am. Chem. Soc.* **1992**, *114*, 9153–9160.
(53) Blades, A. T.; Jayaweera, P.; Ikonomou, M. G.; Kebarle, P. *Int. J. Mass Spectrom. Ion Processes* **1990**, *102*, 251–267.
(54) Luna, A.; Amekraz, B.; Tortajada, J.; Morizur, J. P.; Alcami, M.; Mo, O.; Yanez, M. *J. Am. Chem. Soc.* **1998**, *120*, 5411–5426.
(55) Tsierkezos, N. G.; Schroder, D.; Schwarz, H. *J. Phys. Chem. A* **2003**, *107*, 9575–9581.
(56) Alcami, M.; Luna, A.; Mo, O.; Yanez, M.; Tortajada, J.; Amekraz, B. *Chem. Eur. J.* **2004**, *10*, 2927–2934.
(57) Turecek, F. *Mass Spectrom. Rev.* **2007**, *26*, 563–582.

Scheme 3. CID Mechanism for Loss of Residue 1 in [M − 3H + X]⁻ Complexes[6,52] Yielding x_8 + H for M = OT.
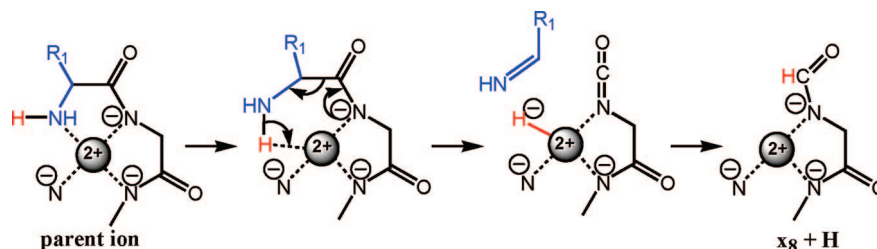
Table 2. Cross Sections (σ in Å^2) and Relative Energies (ΔE in kcal mol^{-1}) for Various Calculated Geometries of Metal−Oxytocin Complexes[a]

	[OT − 3H + Cu]⁻σ_{exp} = 231 Å^2 [b]		[OT + Zn]$^{2+}$$\sigma_{exp}$ = 232 Å^2 [b]	
chelation[c]	4N$_{1689}$	4N$_{1899}$	4O−1N	6O
σ_{calc}[d]	226	245	236	233
ΔE[e]	0.0	21.1	0.0	5.2
Figure	7a	7b	8b	8a

[a] Coordinates of all structures are given in Supporting Information. [b] Experimental cross section. [c] 4N$_{1234}$ denotes chelation by four nitrogen atoms of residues 1, 2, 3, and 4. [d] Calculated cross section is expected to agree with experiment within 3% for reasonable structures. See Methods. [e] Energies derived from full geometry optimizations at the B3LYP/LACVP level.
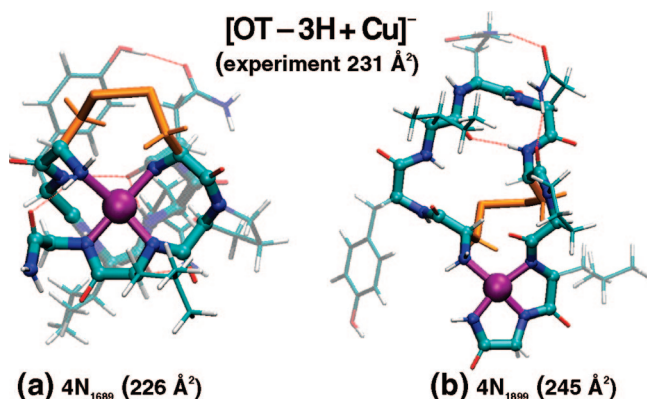
Figure 7. B3LYP/LACVP theoretical structures of [OT − 3H + Cu]⁻ including Cu^{2+} chelation by residues (a) 1, 6, 8, 9 and (b) 1, 8, 9, 9. Cu^{2+} is shown in purple, Cys^1-Cys^6 disulfide bridge in brown. Coordinates of the structures are provided in Supporting Information. Cross sections are given in brackets.
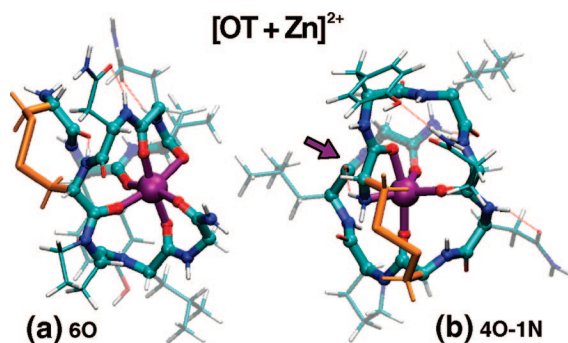
Figure 8. B3LYP/LACVP theoretical structures of [OT + Zn]$^{2+}$ indicating (a) quasi-octahedral and (b) quasi-trigonal-bipyramidal Zn^{2+} chelation. The purple arrow in (b) points to a loosely bound C=O ligand. Coordinates are provided in Supporting Information.

here and shown in Figure 8b. In it the Zn^{2+} ion is coordinated to five backbone carbonyls (one loosely) and the N-terminal

−NH$_2$ group. This structure has a distorted octahedral coordination geometry approaching a trigonal-bipyramidal zinc center (4O−1N coordination). Both, the 6O and the 4O−1N structures agree with the experimental cross section within 2%, indicating that both types of geometries have to be considered reasonable candidate structures.

The exact details of how the OT family of hormones interacts with its cellular receptor protein (OTR) are not known. What is known is that Zn^{2+} potentiates the hormone−receptor interaction and Cu^{2+} does not. These, and other metal ions, could react with either the receptor, the hormone, or both. There is no definitive evidence regarding structural changes in the receptor on metal ion ligation. There is evidence, however, that certain residues play an important role in the interaction,[18,19,58,59] results supported by the high degree of homology in the neurohypophysial family of hormones (Table 1). Of particular interest are OT residues Ile^3, Gln^4, and Asn^5 which are felt to interact with an extracellular loop of OTR.[59] We plot various structures of interest in Figure 9, oriented to show the relative positions of residues 3–5. The [OT + Zn]$^{2+}$ structures have all three residues oriented in approximately the same plane, essential for interaction with a hydrophobic pocket on the receptor.[59] On the other hand, both the metal-free and [OT − 3H + Cu]⁻ structures have very different Ile^3-Gln^4-Asn^5 orientations that would probably not favor binding with a hydrophobic pocket on the receptor. Hence, while no definitive conclusions can be drawn, the results presented here are consistent with the observed facts that Zn^{2+} potentiates receptor interaction and Cu^{2+} does not, based on the very different structures these metal ions induce in the OT hormone.

Conclusions

1. ESI mass spectra of solutions of the OT and VP families of hormones containing divalent metal ions show exceptionally strong peaks for metal−hormone complexes, indicating a strong affinity of the hormones for divalent metal ions. The metal affinity of the hormones under acidic conditions does not depend strongly on the type of divalent metal ion. However, the mass spectrum of a solution containing a mixture of divalent metal ions under *basic conditions* (pH 10) yields exclusively Cu^{2+}−hormone complexes with Cu^{2+} displacing up to four protons.

2. The mass spectrum of a basic OT (VP) solution containing Ni^{2+} but no Cu^{2+} yields Ni^{2+}−OT complexes with Ni^{2+} displacing up to four protons (analogous to Cu^{2+}−OT). Mass spectra of Co^{2+} and Zn^{2+}-containing solutions do not show any evidence of complex formation under basic conditions. The degree of OT deprotonation in metal−OT complexes and the

(58) Hakala, J. M. L. *Biochem. Biophys. Res. Commun.* **1994**, *202*, 1569–1573.
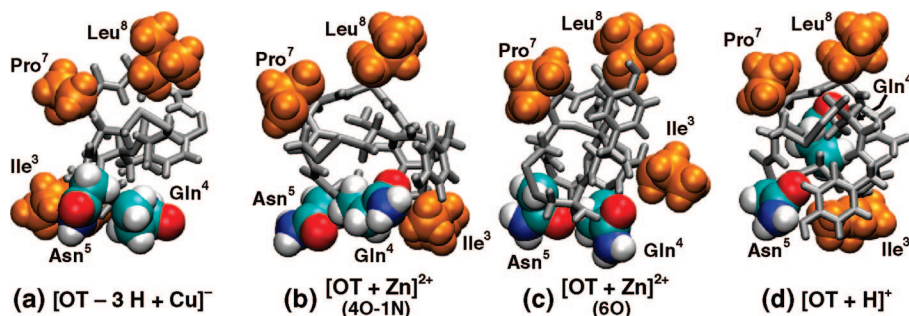(59) Postina, R.; Kojro, E.; Fahrenholz, F. *J. Biol. Chem.* **1996**, *271*, 31593–31601.

Figure 9. Calculated (a) $4N_{1234}$ [OT − 3H + Cu]$^-$, (b) 4O−1N [OT + Zn]$^{2+}$, (c) 6O [OT + Zn]$^{2+}$, and (d) [OT + H]$^+$ structure highlighting the orientation of the side chains of selected residues. Side chains of the hydrophobic residues 3, 7, and 8 are shown in orange/brown. H, C, N, and O atoms of the polar residues 4 and 5 are shown as white, cyan, blue, and red balls, respectively.

propensity for metal−OT complex formation in basic solutions observed by MS ($_{27}$Co, $_{30}$Zn < $_{28}$Ni < $_{29}$Cu) follow qualitatively the same trends established for other peptides by other methods in solution. This result indicates that the transition metal−OT complexes detected following electrospray and desolvation in the mass spectrometer have structures and charges similar to those found in solution.

3. CID experiments on the [OT − 3H + Cu]$^-$ complex yield exclusively C-terminal Cu^{2+}-containing fragments, indicating that Cu^{2+} is bound to the C-terminal side of the peptide.

4. MD and DFT calculations of the [OT + Zn]$^{2+}$ complex yield structures with a pentadentate or hexadentate OT ligand. Both complexes have orientation-averaged cross sections in good agreement with experiment.

5. MD and DFT calculations of the [OT − 3H + Cu]$^-$ complex yield structures with a quasi-square planar Cu^{2+} center and a tetradentate ligand. A low-energy structure with the Cu^{2+} ion bound to deprotonated amide nitrogen atoms of the C-terminal residues Cys^6, Leu^8, and Gly^9 along with the N-terminal amino group has a cross section in good agreement with experiment.

6. The high affinity of OT for divalent metal ions and the rigidity of metal−OT complexes have biological implications with respect to the OT-receptor binding. Possible reasons why Zn^{2+} potentiates OT−OTR binding and Cu^{2+} does not are discussed.

Supporting Information Available: (a) Complete reference 31; (b) comparison of mass spectra recorded in pure water and in a 1:1 water:acetonitrile mixture; (c) mass spectra including CID spectra of IT, VP, and VT; (d) CID mechanisms; (e) ion mobility spectra; (f) coordinates of all geometry-optimized B3YLP/LACVP structures of [OT − 3H + Cu]$^-$, [OT + Zn]$^{2+}$, and [OT + H]$^+$; (e) 8 PDB files. This material is available free of charge via the Internet at http://pubs.acs.org.

JA8002342